ACS APPLIED MATERIALS & INTERFACES

Research Article

www.acsami.org

Electrically Templated Dewetting of a UV-Curable Prepolymer Film for the Fabrication of a Concave Microlens Array with Well-Defined Curvature

Xiangming Li, Hongmiao Tian, Yucheng Ding,* Jinyou Shao,* and Yuping Wei

Micro- and Nano-manufacturing Research Center, State Key Laboratory for Manufacturing Systems Engineering, Xi'an Jiaotong University, 28 Xianning Road, Xi'an 710049, People's Republic of China

Supporting Information

ABSTRACT: This paper presents an economic method, based on electrically templated dewetting of a UV-curable prepolymer, for fabricating a concave microlens array (MLA) of high quality and high density. In our strategy, a voltage is applied to an electrode pair consisting of a conductive substrate coated with a UV-curable prepolymer film and a microhole-arrayed silicon template, sandwiching an air gap, to dewet the prepolymer film into a curved air−liquid interface. At or beyond a critical voltage, the curved prepolymer can be pulled quickly into contact with the protrusive underside of the silicon template. Contact of the prepolymer with the template can be detected by monitoring the leaky current in the polymer, followed by a UV curing of the prepolymer. Finally, by separating the mold from the solidified polymer, a concave MLA is obtained. The curvature of the MLA can be well-defined simply by changing the air gap between the mold and prepolymer film. Besides, the dewetting strategy results in a much smaller adhesion area between the mold and solidified polymer structures, which allows for easy separation of the mold from the MLA in a large-area operation.

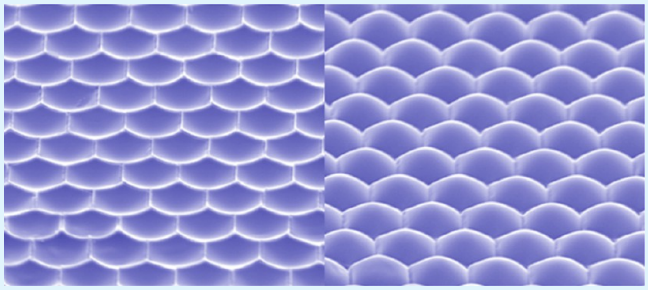

KEYWORDS: *electrically induced dewetting, microlens array, microhole-arrayed template, electrohydrodynamics*

1. INTRODUCTION

Microlenses or microlens arrays (MLAs) have been widely used in microelectromechanical systems, semiconductor solar cells, light-emitting diodes (LEDs), and sensors. For example, the use of MLAs[1−8] had been implemented in both III-Nitride LEDs and organic LEDs, which had been shown to be crucial in improving light extraction and engineering far-field pattern radiation. Obviously, process economy, well-controlled curvature, and smooth surface are quite desirable in the fabrication of MLAs for commercial applications. Laser ablation, ion-beam milling, and other material microremoving processes can produce optics structures with well-controlled shapes[9,10] but may not be suitable for mass application because of the poor cost effectiveness or the poor surface smoothness that results from cascaded material removal. The use of a colloidal-based method or a colloidal lithography technique, based on the assembly or deposition of polystyrene or SiO_2 spheres with micro/nanometer size, had been shown to effectively form the convex-shaped MLAs over a large area.[1−6] The importance of refractive indices,[5,6] dimensions,[2,5] and aspect ratios[1] of such MLAs has proven to be very important in determining the optimized light extraction and far-field patterns in device configurations. In addition, the imprinting method, using the colloidal spheres as a template, had also been used to fabricate concave MLAs in LEDs[7] and organic LEDs.[8] However, it is difficult to precisely control the assembly or deposition of colloidal spheres for generation of a discretionary array of microlens.[11] Thermal reflow techniques[12−14] and a hot embossing method,[15,16] based on interfacial-tension-induced deformation of the photoresist, sol−gel glass, or other thermoplastic polymers, have been used to fabricate MLAs of high surface smoothness economically. However, these thermal approaches are faced with the difficulty of gaining a consistency in the lens surface geometry or focal length. Recently, the formation of adaptive or tunable focal liquid lenses, based on electrowetting actuation,[17,18] liquid dielectrophoresis,[19] or thermal response of liquid microdroplets,[20] has shown good controllability in the curvature or focal length of a lens by electric field or heating. However, it can be very difficult (if possible) for these processes to form arrayed microlenses with a high fill factor and a stable curvature over a large area because of the nature of droplet-wise manipulation, which often causes a merging of the neighboring droplets, and because of electrothermally induced liquid evaporation, which tends to cause a volumetric shrinkage of the droplets during a long-time operation.

Received: May 28, 2013
Accepted: July 31, 2013
Published: July 31, 2013

 © 2013 American Chemical Society dx.doi.org/10.1021/am402043u | ACS Appl. Mater. Interfaces 2013, 5, 9975−9982

More recently, a pattern-modulated electric field was also used to fabricate solid MLAs by a number of researches.[21−23] On the basis of the electrohydrodynamic instability (EHDI) of a liquid film under a spatially modulated electric field, an approach for generating MLAs was proposed, starting with formation of an array of liquid bridges between a pair of electrodes.[21] Upon separation of the micropatterned electrode from the substrate electrode, the liquid bridges were broken and a microdroplet array was formed on the substrate, which were then cured to form a solidified MLA. The process was more like a strategy to quickly generate a microdroplet array from a liquid film via EHDI. Obviously, the geometry of the generated droplets could not be reshaped anymore, and it was also difficult to achieve a high fill factor (less than 40% in their experiments) because of the difficulty of obtaining a high density of liquid bridges by EHDI. In order to form solidified MLAs with well-controllable curvature, improved alternatives were proposed, in which a droplet array of polymer (such as SU-8) was premeditatedly generated onto an indium−tin oxide (ITO)/glass substrate,[22,23] and then a voltage was applied between the substrate and an upper planar electrode to electrically pull droplets into desired shapes. However, the droplets can be electrohydrodynamically deformed in such a way as to reach the upper electrode once the electric field is higher than a critical level, resulting in a microlenses with a flat top or even an undesirable merging of neighboring droplets because of their instability under a strong electric field.[21]

It should be indicated that most of the previous attempts were made to generate MLAs with *convex* curvature, and relatively fewer efforts[24,25] were carried on for directly fabricating *concave* MLAs, which have unique applications, such as compound refractive lenses for focusing X-rays, DNA chip carriers, diffusers in LEDs, and so forth.[26−28]

In previous research by the current authors,[25] concave MLAs were generated by electrowetting a dielectric UV-curable prepolymer on the inner wall of microholes arrayed on a conductive template. A prepolymer film coated on a conductive substrate was trapped intentionally with air in the deep microholes by mechanically pressing a microhole-arrayed template against the substrate. The subsequent application of a voltage between the template and substrate caused the top surface of the incompletely filled prepolymer to be deformed into a concave meniscus with a voltage-dependent curvature due to an electrowetting of the liquid prepolymer on the microhole wall. In the process, a large pressure would be required to trap the prepolymer film with air into the microholes, especially for fabrication of a large area MLA, which may not be desirable for some brittle substrate. Furthermore, owing to wetting of the prepolymer to the microhole wall, the adhesion area between the solidified polymer and microhole wall can also cause difficulty in removing the template, especially for concave MLAs with large curvature.

This paper presents a new approach for economically fabricating *concave* MLA based on electrically templated dewetting of a UV-curable liquid prepolymer film, by using a microhole-arrayed template, which produces a spatially modulated electric field on the initially flat prepolymer film. Beyond a criticle voltage, the corresponding Maxwell pressure on the prepolymer film surface (i.e., the air−liquid interface) pulls the prepolymer into a final contact with the upper protrusive underside of the template, leaving prepolymer valleys under the holes of the template. The curvature of the formed valleys is then independent of the voltage but can be well tunned by simply varying the initial air gap between the template and prepolymer film. Because the actual prepolymer−template contact only happens on the template's protrusion, which makes up only a small portion of the template's projected area, the approach allows for easy removal of the template from the solidified prepolymer valleys (i.e., MLA) because of a reduced adhesion area. Also, because the template is initially separated from the prepolymer surface by an air gap, no large pressure is needed to preload the substrate, which is desirable for fabricating a large-area concave MLA, especially on a brittle substrate.

2. EXPERIMENTAL DETAILS

2.1. Method. Figure 1 illustrates the process of electrically templated dewetting for generating a concave MLA. A UV-curable

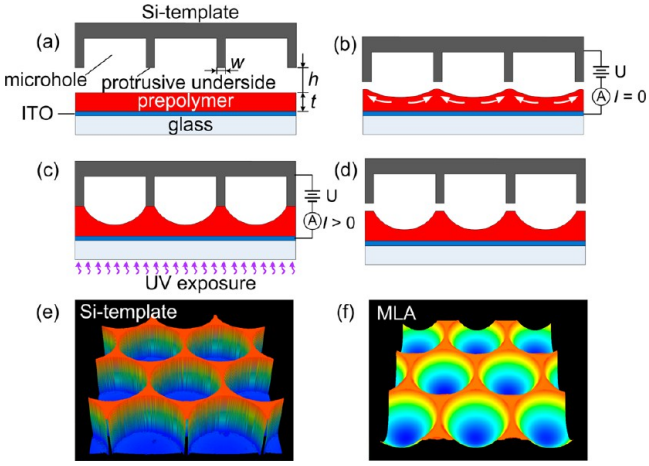

Figure 1. Illustration of the electrically templated dewetting process for generation of concave MLAs: (a) a microhole-arrayed silicon template is separated from the liquid prepolymer (with a thickness t) by an air gap h; (b) a dc voltage is applied between the silicon template and ITO/glass substrate to electrically dewet the initially flat prepolymer film (with the arrows indicating the flowing directions of the prepolymer), and the leaking current is monitored between the substrate and template; (c) the prepolymer rises into a final contact with the protrusive underside of the silicon template (a microampere scale leaking current through the prepolymer, I, can then be detected) and is cured by UV exposure; (d) removal of the template leads to a solidified concave MLA. (e and f) Experimentally measured 3D profiles of the template arrayed with cylindrical microholes and the corresponding concave MLA, respectively (acquired by LSCM).

prepolymer (mechanically in a state of liquid) with proper light transmission and refraction is spin-coated into a film of proper thickness on an ITO/glass substrate. A microhole-arrayed silicon template, which is doped for a proper electric conductivity and fabricated by conventional photolithography and plasma etching, is placed over the prepolymer film with a proper air gap (Figure 1a). In our practical experiment, the air gap was adjusted by properly distributed glass spacers, which were sandwiched between the template and substrate. When a sufficiently large voltage is applied between the template and substrate, a nonuniformly distributed Maxwell pressure due to the microhole-array-templated electric field tends to dewet the initially flat prepolymer film so that the prepolymer below the protrusive underside of the template rises upward (Figure 1b). A global leaking current of the dielectric prepolymer is monitored and used to judge a proper contact of the prepolymer with the template underside. This detectable polymer−template contact is, in turn, used to trigger a switch-off of the voltage and a switch-on of the UV

exposure (Figure 1c). Finally, a concave MLA is obtained by removing the template from the substrate (Figure 1d). In our experiment, the silicon template was hexagonally arrayed with cylindrical microholes of 100 μm diameter, 150 μm depth, and 104 μm center distance of each two neighboring microholes, as experimentally acquired by laser scanning confocal microscopy (LSCM) and shown in Figure 1e. The minimum thickness for the wall of microholes is 4 μm.

2.2. Materials and Equipment. The ITO layer on a glass substrate was sputtered by a Denton Vacuum Explorer14 sputterer. The UV-curable prepolymer was an acrylic-based compound liquid, available from Micro Resist Technology GmbH (with a commercial name OrmoComp), which has a viscosity of 0.41 Pa·s and a dielectric constant of roughly 6.8 at room temperature. The direct-current (dc) voltage were supplied by an arbitrary-waveform generator (AGILENT-ER 33220A), which was bridged by an amplifier/controller (TREK 610E HV) to the template and ITO substrate. The leaking current in the prepolymer is in site monitored using an oscillograph (Tektronix DPO3034). The voltage supply/amperemeter on the AGILENTER 33220A and UV-light control were interface to a PC, which could precisely sequence switching of the voltage and initiation of UV curing. The silicon template are made of a n-type-doped silicon wafer, which has an electric resistivity of ≈0.005−0.015 Ω·cm. For easy detemplating, the silicon template was treated in a 1.0 wt % ethanol solution of (heptadecafluorodecyl)trimethoxysilane [$CF_3(CF_2)_7CH_2CH_2Si(OCH_3)_3$, FAS] for 3 h and subsequently baked at 150 °C for 10 h. The master of concave MLA (for duplicating a convex MLA by a vacuum microtemplateing process) was coated with an antiadhesive fluoropolymer in an ICP-CVD chamber (Oxford ICP-180). The SEM images were obtained by using a Hitachi SU8010. The cross section and 3D profiles of MLAs were obtained by LSCM (Olympus OLS4000). The roughness of the sag surface of the microlens was measured by a Veeco Innova atomic force microscope. The imaging and focusing performances of MLA were tested by using an optical microscope (KEYENCE VH-8000).

3. RESULTS AND DISCUSSION

3.1. Electrically Templated Dewetting. A structured template, working as an electrode, can generate a spatially modulated electric field, which leads to nonuniform Maxwell tension on the surface of the initially flat prepolymer film. The nonuniform Maxwell tension tends to destabilize the flat liquid film under the template and allows for polymer deformation into a shape depending on the spatial distribution of the electric field. This electrically induced process has been widely addressed as a patterning technique for generating various functional micro/nanostructures.[29−32] Figure 2 experimentally shows 3D deformation of the prepolymer caused by electrically templated dewetting of the prepolymer film under different voltages, which all sustained for 10 s in our experiment. The initially flat prepolymer film interfaced with air becomes unstable under a nonuniformly distributed electric field, and the prepolymer tends to collect preferably toward the protrusive underside of the template, where the electric field has the highest intensity,[33−35] leading to dewetting of the prepolymer. While the dewetting prepolymer rises toward the protrusive underside of the template, the prepolymer below the underside of each microhole tends to sink into a valley to maintain a hydraulic continuity. The rising height of the dewetting prepolymer is determined by the equilibrium between the voltage-dependent Maxwell pressure and a resultant of the curvature-dependent surface tension and the viscous resistance.[36] Therefore, the curvature for the arrayed valleys is strongly dependent on the applied voltage, as shown in Figure 2a−c for the polymer surface profiles and in Figure 2e for the profiles of a polymer cross section at different voltages.

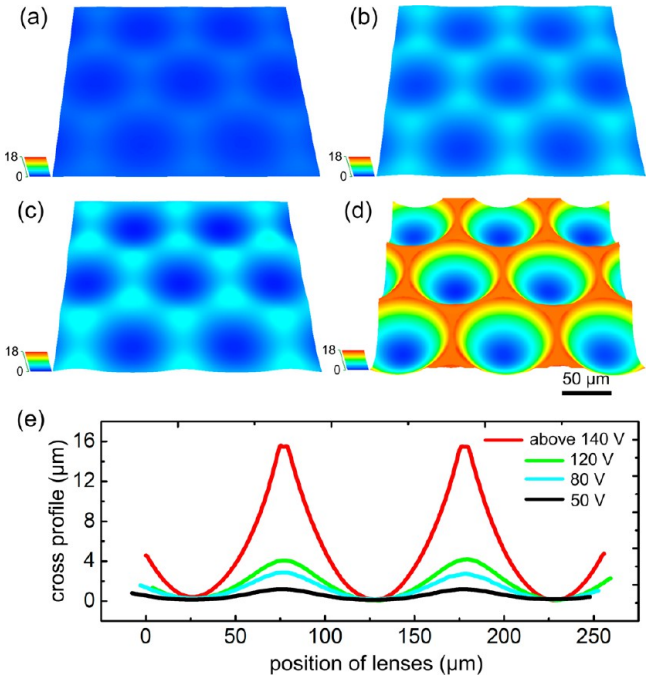

Figure 2. Experimentally measured profiles of the deformed prepolymer film at different voltages: (a−d) LSCM-acquired 3D topographies of the deformed prepolymer film at voltages of 50, 80, 120, and 140 V, respectively (the color-coded height is in units of micrometers); (e) profiles of a cross section of the deformed prepolymer film for the corresponding voltages.

It is interesting to see from Figure 2a−c that for each of the voltages the prepolymer rises to the highest point below the widest spots of the template's protrusive underside. This can be explained by the fact that the lowest surface tension of the air−liquid interface (therefore, a low resistance against the prepolymer's rise) is produced under these widest spots of the protrusive underside for any rising height. Therefore, the electrodewetting process tends to produce arrayed valleys with six horns hexagonally located around each valley if a template arrayed hexagonally with microholes is used, as shown clearly in Figure 2c.

However, if a sufficiently large voltage is applied, 140 V or larger, for instance, the dewetting prepolymer can finally rise to reach the protrusive underside of the template, leading to a maximum curvature for the arrayed valleys (i.e., a concave MLA with well-defined shape), as shown in Figure 2d. It should be mentioned that, in our experiments, the voltage was switched off according to the monitored current before UV exposure was switched on, where the necessity will be explained in the following. When the electric field vanishes, such a curvature of the valleys can be expected to be sustained because the contact between the prepolymer and the template's protrusive underside will be maintained by the liquid−solid adhesion.[37,38] As a result, detection for the liquid−solid contact becomes important to allow for generation of a concave MLA with well-defined curvature.

3.2. Leaky Current through the Prepolymer. Many liquid prepolymer compounds, such as the one used in our experiment, are leaky dielectric, and a weak and transient conductivity can be expected because of charge carriers, such as free ions, spare electrons, and polarized charges, inherent in the prepolymer,[39−41] causing a leaking current (usually in a microampere scale) under an externally applied electrical

field. This leaking current can jump to a maximum because of an electrical conduction generated by the charge carrier when the prepolymer rises into full contact with the template's protrusive underside. Therefore, in site monitoring of this leaking current can be performed to identify the contacting state of the prepolymer and template underside.

Figure 3a shows the leaking current experimentally monitored during formation of a MLA at a dc voltage of 140 V, which was sustained without UV curing. It is interesting to note that, once the leaking current jumps to a maximum (because of full contact of the prepolymer with the conductive template underside protrusions[42]), it is immediately followed by a continuous decline to a nonzero constant. The declining leaking current after a maximum can be attributed to electrical conduction by the polarized charges, which vanish with time during charging of the capacitor, which is made of the template and substrate as an electrode pair. The nonzero constant leaking current is due to conduction by the leaky charge in the prepolymer compound. Most importantly, the initially sharp decline in the leaking current, as a lucky coincidence, makes it easy to spot a timing for the maximum from a noise-contaminated current signal and therefore to identify a timing for the prepolymer–template contact.

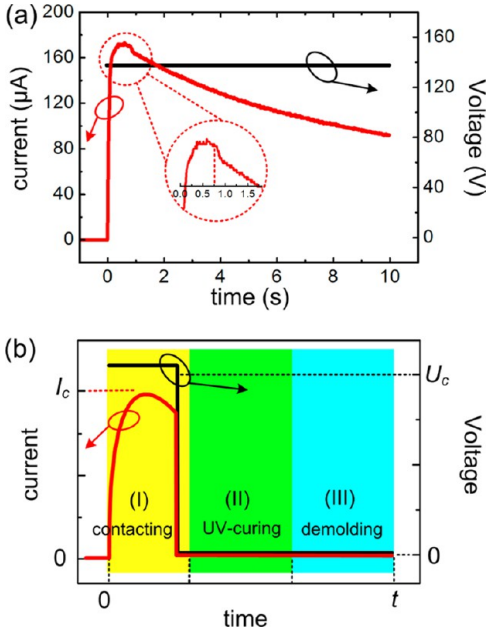

Figure 3. (a) Characteristics of the prepolymer's leaking current experimentally monitored in an electrically templated dewetting process (for a microhole-arrayed silicon template squired at 25 mm × 25 mm and a voltage of 140 V). Note that the leaking current starts to declines within 1 s, as indicated in the inset. (b) Illustrative timing for voltage switching off and UV-curing switching on, with I–III representing the time zone of the prepolymer–template contact, UV curing, and template removal, respectively. U_c is the critical voltage that can produce a Maxwell pressure large enough to pull the dewetting prepolymer to reach the protrusive underside of the template, and I_c is the maximum leaking current.

It is important to mention that, once the liquid prepolymer rises into a proper contact with the template, a sustaining voltage is not desirable. This is because the prepolymer already in contact with the template's protrusive underside may further electrowet the inner wall of microholes when the large voltage is sustaining, causing problems for subsequent removal of the template from the UV-cured MLA. More importantly, because the electric field at the valley surface is so strong and not rotationally symmetrical that the valley shape tends to be unstable and shows a nonrevolution surface, a poor surface quality will be formed (see Supporting Information Figure S1). In order to avoid such drawbacks caused by the electric field, a time sequencing is proposed for switch-off of the voltage and switch-on of UV exposure based on the leaking current, as illustrated in Figure 3b. Once a sharp drop in the leaking current is detected, it triggers a switch-off of the voltage and a delayed switch-on of UV curing. The delay between the voltage switch-off and UV-curing switch-on was taken as 100–300 ms in our experiment, depending on the voltage applied. The delayed initiation of UV curing allows for the voltage-dependent Maxwell pressure on each prepolymer valley to vanish and the electrohydrodynamically deformed prepolymer surface to be restored to a shape predominantly determined by the surface tension.

3.3. Curvature of the Prepolymer Valley. Figure 4 shows the SEM images of concave MLAs generated at the different air gap h and initial prepolymer thickness t. In order to produce a Maxwell pressure large enough to pull the prepolymer safely

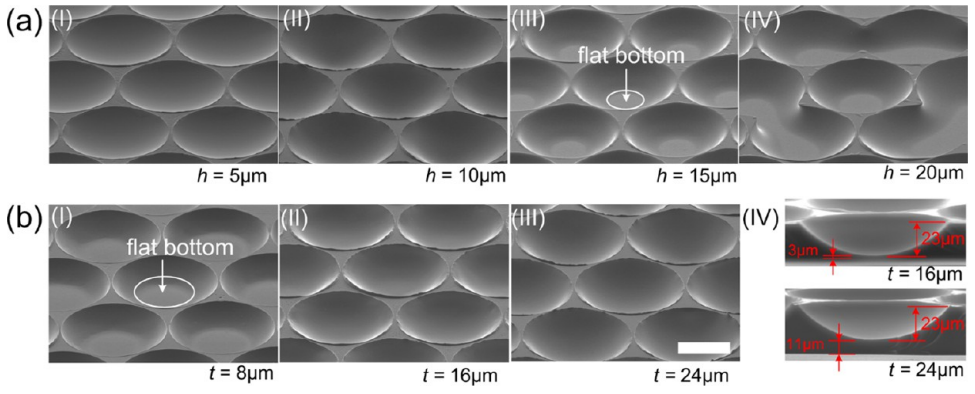

Figure 4. SEM images of concave MLAs fabricated with curvature depending on the air gap h and the prepolymer thickness t at a constant voltage of 300 V: (a) for h varying from 5 to 20 μm while t was fixed at 15 μm; (b) for t varying from 8 to 24 μm while h was fixed at 10 μm. Note that the sag height H is not influenced by the prepolymer thickness t if t is large enough (b-IV shows that a further increase in the prepolymer thickness only leads to a thick valley bottom). Scale bar: 50 μm.

into a contact with the protrusive underside of the template for all of the air gaps and prepolymer thicknesses, intentionally a high voltage of 300 V was used throughout our experimental fabrication of the MLAs shown.

As can be seen in Figure 4a, at a fixed prepolymer thickness (t = 15 μm), the sag height of MLA varies from 12 μm for an air gap of 5 μm (Figure 4a-I) to 23 μm for an air gap of 10 μm (Figure 4a-II), meaning that the MLA curvature tends to increase with the air gap. However, when the air gap increases to 15 μm (Figure 4a-III), flat-bottom valleys are undesirably generated because at this prepolymer thickness the central portion of prepolymer in each valley has to be evacuated so that the prepolymer below the protrusive underside of the template can collect into a volume enough to reach the template. When the air gap h increases further to 20 μm, the prepolymer thickness comparatively becomes too small to provide a sufficient amount of prepolymer to reach the template underside, causing an undesirable merging of neighboring flat-bottom valleys, as shown in Figure 4a-IV.

On the other hand, for a constant air gap (h = 10 μm), a small prepolymer thickness, t = 8 μm, for instance, again leads to flat-bottom valleys, as shown in Figure 4b-I. When the prepolymer thickness becomes large enough, t = 16 μm, for instance, the process produces adequate shape for the MLA, with a sag height of 23 μm, as shown in Figure 4b-II,IV. However, a further increase in the prepolymer thickness will not increase the sag height of the MLA, as shown in Figure 4b-III,IV.

These results suggest that an adequate shape for the concave MLA can be generated only when the prepolymer thickness is large enough to provide a sufficient prepolymer for reaching the template underside.

The microlenes tend to be spherical according to a geometrical fitting to the experimentally measured profiles (see the Supporting Information Figure S2). This can be explained by the force equilibrium and energy minimization. During deformation of the prepolymer film, three kinds of forces are involved, including the Maxwell tensor acting on the polymer surface, surface tension, and gravity of the polymer. Owing to the small size of the microlens, the gravity can be ignored, and because the voltage is switched-off before UV curing of the prepolymer, the Maxwell tensor has vanished. As a result, the shapes of the microlenses depend only on the natural surface tension and tend to be spherical to maintain minimization of the surface energy. When shrinkage due to UV polymerization is ignored, the sag height of concave MLA (with spherical surface), H, can then be determined geometrically by h, t, r, and w, based on a volumetric continuity of the prepolymer shown in Figure 5. Because of the periodically repetitive nature of MLA, only a hexagonal prepolymer film has been taken into consideration. By assuming that the hexagonal prepolymer film with a thickness t is continuously deformed into a spherical bowl with an aperture radius r, which can be taken as being equal to the microhole's radius, a sag height H can be determined by the following geometrical relationship:

$$H(H^2 + 3r^2) = \frac{12\sqrt{3}}{\pi} h\left(r + \frac{w}{2}\right)^2 \quad (1)$$

It can be seen from eq 1 that the sag height H is only determined by the air gap h for a given template. From Figure 5, it can also be seen that the thickness of the prepolymer at the valley bottom is obtained by $b = (h+ t) - H$. In order to avoid a

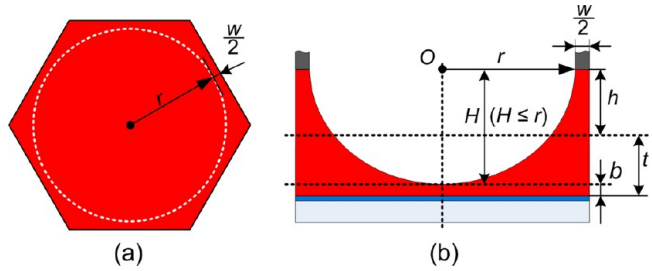

Figure 5. Sag height H versus air gap h: (a) hexagonal prepolymer area under each of the cylindrical microholes hexagonally arrayed on the template (the dotted circle represents the projection of a microhole); (b) parameters of the valley.

flat-bottom valley, b should be greater than zero. Therefore, the initial prepolymer thickness, t, should be determined in terms of the air gap h by the inequality as $t > H - h$. For microlenses of spheres with given apertures, the radius of curvature (R) depends only on the sag height, i.e., $R = (1/2)(H + r^2/H)$. In theory, the radius of curvature can range from R = 50 μm (for h = 27.9 μm, and the initial polymer film is thick enough, i.e., larger than 22.1 μm, as in our experiment) to $R \rightarrow +\infty$ (when $h \rightarrow 0$).

3.4. Density of *Cancave* MLA and Its Duplicated *Convex* MLA. The fill factor or density of the MLA is determined by the density of microholes arrayed on the template. A high density of microholes in a template, which tends to result in a large electric field contrast in spatial distribution, can be easily and precisely achieved by the conventional silicon microfabricating process (i.e., photolithography and dry etching on a silicon wafer) with a minimized wall thickness. Figure 6 shows a MLA of a

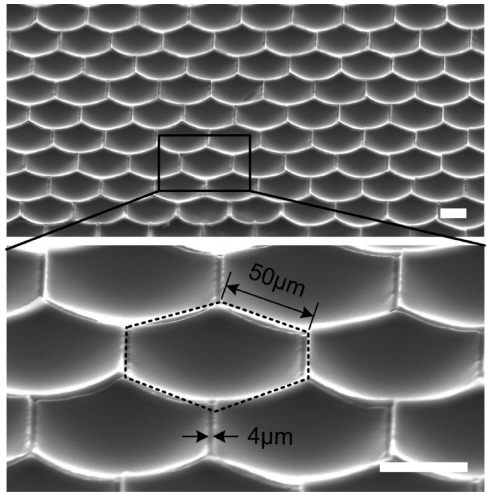

Figure 6. SEM images of a concave MLA with a hexagonal aperture. Scale bar: 50 μm.

hexagonal aperture fabricated by the electrically templated dewetting process, which has a fill factor calculated as high as up to 93%.[25] However, in order to maintain the mechanical strength of the microhole wall and to avoid the electric spark that can be induced by a thin wall, the thickness of the wall should be selected empirically as 0.5 μm and above. As a result, the corresponding maximum fill factor is 98.8% for the hexagonally arrayed microlenses with a hexagonal aperture and 89.8% for the hexagonally arrayed microlenses with a

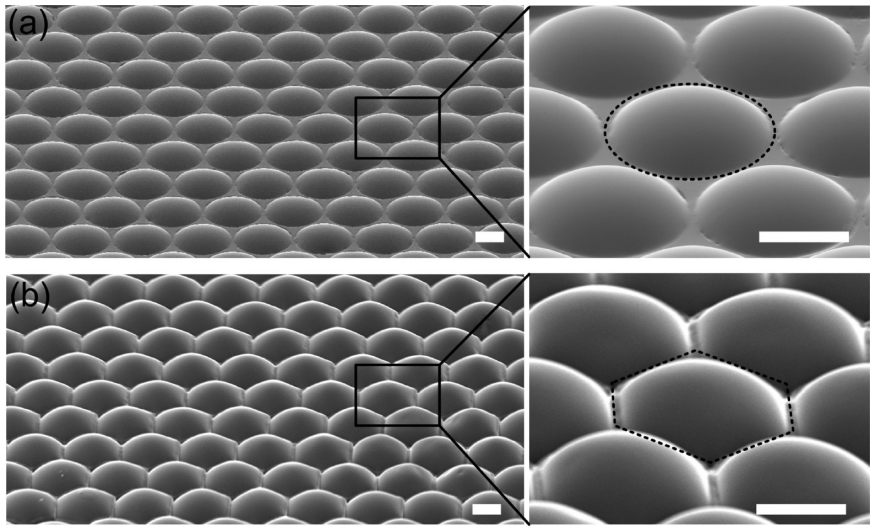

Figure 7. SEM images of convex MLAs duplicated by using the concave MLAs shown in Figure 4a-II and Figure 6 as the masters: (a) convex MLA with a circular aperture; (b) convex MLA with a hexagonal aperture. Scale bar: 50 μm.

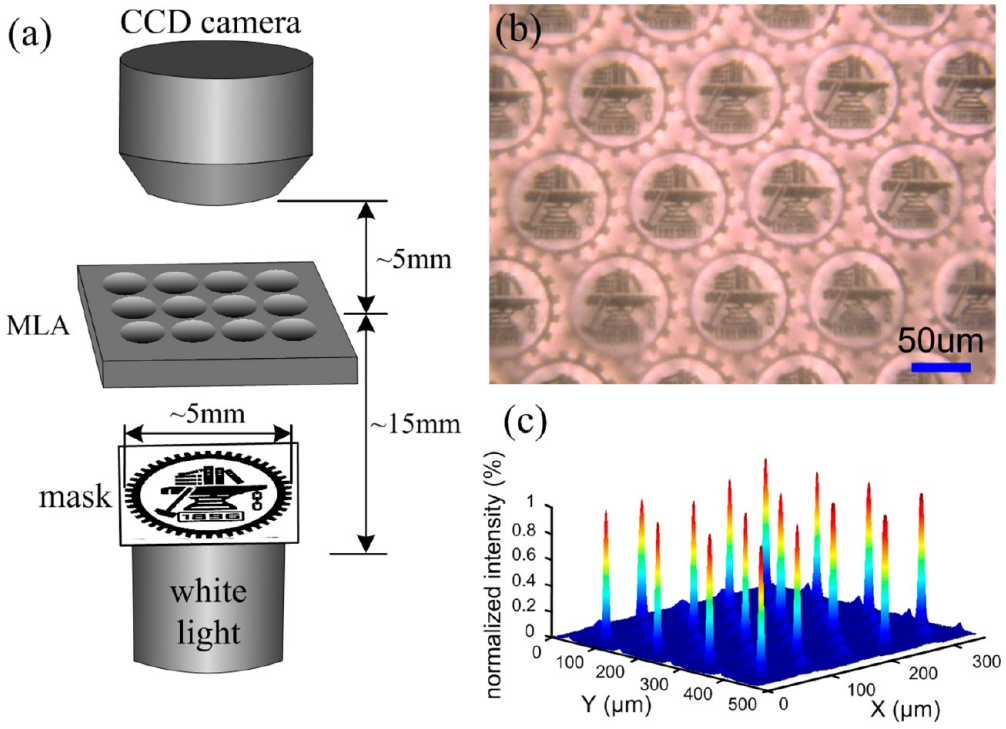

Figure 8. Test for the optical properties of concave MLA: (a) diagram of the optical microscopic setup to evaluate imaging and focusing performances of the MLA; (b) image of the authors' school badge obtained by using a concave MLA with a sag height of ~12 μm; (c) measured light intensity profiles of a concave MLA with a sag height of ~23 μm.

circular aperture, at the best, as estimated by an equation.[25] Because the high density corresponds to a reduced global area for the template's protrusive underside contacting with the prepolymer, an increase in the density is also desirable for reducing the polymer−template adhesion for easier removal of the template from the cured MLA.

In addition, the surface roughness of microlenses is also an important parameter for optical applications. The roughness was measured by atomic force microscopy over an area of 2 μm × 2 μm as R_a = 0.2 nm, which is much smaller than that for a surface fabricated by laser ablation or other material removal process.[43] The aspect ratio of a microlens, i.e., ratio of the sag height to the aperture diameter, is also an important parameter for MLAs. In order to achieve a higher aspect ratio, a properly large air gap (h) is preferable between the template and initial prepolymer film with a sufficient thickness (t), according to eq 1. In theory, the maximum aspect ratio can reach 0.5 when the microlens surface turns into a complete semisphere.

The concave polymer MLA generated by the proposed process either is optically functional or can be further used as a master to produce a convex MLA by a vacuum micro-templateing process.[17] Figure 7 shows the convex MLAs with circular (Figure 7a) and hexagonal (Figure 7b) apertures, duplicated by using the concave MLAs.

3.5. Test of Optical Performances of MLAs. Figure 8 shows the optical performance of concave MLAs fabricated by our strategy. Figure 8a illustrates the setup that we used for testing the focusing and imaging properties of the MLAs. First, a concave MLA was positioned horizontally on a motion stage and moved relative to a CCD camera. The MLA was illuminated with a white light from behind a mask with a pattern of our school badge, which was fabricated by laser ablation of a chromium film sputtered on a slide glass. On the false image plane of the concave MLA, an array of bright false and reduced images of the school badge could be clearly observed on the CCD camera (Figure 8b). When a mask with an optical aperture (3 mm in diameter) was used instead, sharply focused spots on the false focal plane of the MLA could be obtained, with the uniform light intensity shown in Figure 8c.

4. CONCLUSION

The approach described in this paper for generating concave MLA has some desirable and unique features for industrial application, including process cost effectiveness due to the ease with which a microhole-arrayed silicon template can be economically fabricated by the conventional microfabrication technology, a high efficiency due to the capability of producing large-area MLAs without the need for a large preload on the substrate, and, most importantly, an exact controllability of the curvature due to the fact that the curvature for a concave MLA to be generated can be predetermined by its simple and geometrical relationship to the air gap and prepolymer thickness.

■ ASSOCIATED CONTENT

Supporting Information

SEM images of a concave valley array and a concave MLA, which were formed by different voltages during UV curing of the prepolymer, and spherical fitting result of a microlens generated by electrically templated dewetting. This material is available free of charge via the Internet at http://pubs.acs.org.

■ AUTHOR INFORMATION

Corresponding Author

*E-mail: ycding@mail.xjtu.edu.cn (Y.D.), jyshao@mail.xjtu.edu.cn (J.S.).

Notes

The authors declare no competing financial interest.

■ ACKNOWLEDGMENTS

X.L. and H.T., two Ph.D. candidates of the corresponding authors, have contributed equally to this work, which is financed by the Major Research Plan of NSFC on Nanomanufacturing (Grant 90923040), NSFC Funds (Grants 51005178 and 51175417), the National Basic Research Program of China (Grant 2009CB724202), and China's "863" Program (Grant 2012AA041004).

■ REFERENCES

(1) Li, X. H.; Song, R. B.; Ee, Y. K.; Kumnorkaew, P.; Gilchrist, J. F.; Tansu, N. *IEEE Photonics J.* **2011**, *3*, 489−499.
(2) Ee, Y. K.; Kumnorkaew, P.; Arif, R. A.; Tong, H.; Zhao, H. P.; Gilchrist, J. F.; Tansu, N. *IEEE J. Sel. Top. Quantum Electron.* **2009**, *15*, 1218−1225.
(3) Kang, E. K.; Song, Y. M.; Jang, S. J.; Yeo, C. I.; Lee, Y. T. *IEEE Photonics Technol. Lett.* **2013**, *25*, 1118−1121.
(4) Galeotti, F.; Mróz, W.; Scavia, G.; Botta, C. *Org. Electron.* **2013**, *14*, 212−218.
(5) Zhu, P.; Liu, G.; Zhang, J.; Tansu, N. *J. Disp. Technol.* **2013**, *9*, 317−323.
(6) Li, X.-H.; Zhu, P.; Liu, G.; Zhang, J.; Song, R.; Ee, Y.-K.; Kumnorkaew, P.; Gilchrist, J. F.; Tansu, N. *J. Disp. Technol.* **2013**, *9*, 324−332.
(7) Ee, Y.-K.; Kumnorkaew, P.; Arif, R. A.; Tong, H.; Gilchrist, J. F.; Tansu, N. *Opt. Express* **2009**, *17*, 13747−13757.
(8) Koo, W. H.; Youn, W.; Zhu, P. F.; Li, X. H.; Tansu, N.; So, F. *Adv. Funct. Mater.* **2012**, *22*, 3454−3459.
(9) Fu, Y.; Kok, N.; Bryan, A. *Microelectron. Eng.* **2000**, *54*, 211−221.
(10) Brodoceanu, D.; Cole, G. D.; Kiesel, N.; Aspelmeyer, M.; Bäuerle, D. *Appl. Phys. Lett.* **2010**, *97*, 041104.
(11) Kumnorkaew, P.; Ee, Y.-K.; Tansu, N.; Gilchrist, J. F. *Langmuir* **2008**, *24*, 12150−12157.
(12) He, M.; Yuan, X. C.; Ngo, N. Q.; Bu, J.; Kudryashov, V. *Opt. Lett.* **2003**, *28*, 731−733.
(13) Yang, H.; Chao, C. K.; Wei, M. K.; Lin, C. P. *J. Micromech. Microeng.* **2004**, *14*, 1197.
(14) Lu, Y.; Yin, Y.; Xia, Y. *Adv. Mater.* **2001**, *13*, 34−37.
(15) Yabu, H.; Shimomura, M. *Langmuir* **2005**, *21*, 1709−1711.
(16) Kunnavakkam, M. V.; Houlihan, F. M.; Schlax, M.; Liddle, J. A.; Kolodner, P.; Nalamasu, O.; Rogers, J. A. *Appl. Phys. Lett.* **2003**, *82*, 1152.
(17) Krupenkin, T.; Yang, S.; Mach, P. *Appl. Phys. Lett.* **2003**, *82*, 316.
(18) Yang, S.; Krupenkin, T. N.; Mach, P.; Changdross, E. A. *Adv. Mater.* **2003**, *15*, 940−943.
(19) Ren, H.; Wu, S.-T. *Opt. Express* **2008**, *16*, 2646−2652.
(20) Dong, L.; Agarwal, A. K.; Beebe, D. J.; Jiang, H. *Adv. Mater.* **2007**, *19*, 401−405.
(21) Lee, Y.-J.; Kim, Y. W.; Kim, Y.-K.; Yu, C.-J.; Gwag, J. S.; Kim, J.-H. *Opt. Express* **2011**, *19*, 10673−10678.
(22) Kuo, S.-M.; Lin, C.-H. *Opt. Express* **2010**, *18*, 19114−19119.
(23) Wei, H.-C.; Su, G.-D. *J. Micromech. Microeng.* **2012**, *22*, 025007.
(24) Li, X.; Ding, Y.; Shao, J.; Liu, H.; Tian, H. *Opt. Lett.* **2011**, *36*, 4083−4085.
(25) Li, X.; Ding, Y.; Shao, J.; Tian, H.; Liu, H. *Adv. Mater.* **2012**, *24*, OP165−OP169.
(26) Snigirev, A.; Kohn, V.; Snigireva, I.; Lengeler, B. *Nature* **1996**, *384*, 49−51.
(27) Schena, M.; Shalon, D.; Davis, R. W.; Brown, P. O. *Science* **1995**, *270*, 467−470.
(28) Ruffieux, P.; Scharf, T.; Philipoussis, I.; Herzig, H. P.; Voelkel, R.; Weible, K. J. *Opt. Express* **2008**, *16*, 19541−19549.
(29) Schäffer, E.; Thurn-Albrecht, T.; Russell, T. P.; Steiner, U. *Nature* **2000**, *403*, 874−877.
(30) Tian, H.; Ding, Y.; Shao, J.; Li, X.; Liu, H. *Soft Matter* **2013**, *9*, 6564−6564.
(31) Goldberg-Oppenheimer, P.; Mahajan, S.; Steiner, U. *Adv. Mater.* **2012**, *24*, OP175−OP180.
(32) Li, X.; Shao, J.; Ding, Y.; Tian, H.; Liu, H.. *J. Micromech. Microeng.* **2011**, *21*, 115004.
(33) Tian, H.; Shao, J.; Ding, Y.; Li, X.; Li, X. M. *Electrophoresis* **2011**, *32*, 2245−2252.
(34) Tian, H.; Shao, J.; Ding, Y.; Li, X.; Li, X. M.; Liu, H. *J. Vac. Sci. Technol. B* **2011**, *29*, 041606.
(35) Castellanos, A. *Electrohydrodynamics*; Springer-Verlag: New York, 1998; Chapter 8, p 134.
(36) Yang, Q.; Ben Q.; Li; Ding, Y. *Soft Matter* **2013**, *9*, 3412−3423.
(37) Voïtchovsky, K.; Kuna, J. J.; Contera, S. A.; Tosatti, E.; Stellacci, F. *Nat. Nanotechnol.* **2010**, *5*, 401−405.
(38) Liu, M.; Jiang, L. *Adv. Funct. Mater.* **2010**, *20*, 3753−3764.
(39) Saville, D. A. *Annu. Rev. Fluid Mech.* **1997**, *29*, 27−64.
(40) Bentenitis, N.; Krause, S. *Langmuir* **2005**, *21*, 6194−6209.
(41) Suh, K. S.; Yoon, H. G.; Lee, C. R.; Okamoto, T.; Takada, T. *IEEE Trans. Dielectr. Electr. Insul.* **1999**, *6*, 282−287.
(42) Goldberg-Oppenheimer, P.; Steiner, U. *Small* **2010**, *6*, 1248−1254.

(43) Chen, F.; Liu, H.; Yang, Q.; Wang, X.; Hou, C.; Bian, H.; Liang, W.; Si, J.; Hou, X. *Opt. Express* **2010**, *18*, 20334−20343.